Available online at www.sciencedirect.com
SCIENCE DIRECT
Catalysis Today 113 (2006) 240–244
CATALYSIS TODAY
www.elsevier.com/locate/cattod

$Zn_{1-x}Co_xO$ diluted magnetic semiconductors synthesized under hydrothermal conditions

M. Bouloudenine [a,b], N. Viart [a], S. Colis [a], A. Dinia [a,*]

[a] *Institut de Physique et Chimie des Matériaux de Strasbourg, IPCMS, Groupe des Matériaux Inorganiques, CNRS-UMR 7504, ULP-ECPM, 23 Rue du Loess, BP 43, F-67034 Strasbourg Cedex 2, France*
[b] *Université de Annaba, Faculté des Sciences, Département de Physique, BP 12, Annaba 23000, Algeria*

Available online 6 January 2006

Abstract

Polycrystalline $Zn_{1-x}Co_xO$ magnetic semiconductors were synthesized by hydrothermal technique from aqueous solutions of Zn and Co acetates using potassium hydroxide KOH as hydrolytic catalyst. The structural and magnetic properties of the samples were investigated as a function of acetates and KOH concentrations. The results show that the highest amount of Co that can be successfully inserted in the ZnO matrix is around 10%, when using concentrations of 0.5 and 0.77 mol/L of acetate and KOH, respectively. For the $Zn_{0.9}Co_{0.1}O$ sample, X-ray diffraction indicates a pure ZnO würtzite structure free of parasitic phases in agreement with optical measurements that reveal the presence of Co^{2+} cations in substitution of Zn^{2+}. The magnetization measurements show a paramagnetic behaviour and no evidence of ferromagnetism. This may be due to the absence of free carriers.

PACS: 78.40.−q; 75.50.Pp; 81.30.Mh

Keywords: Magnetic semiconductor; Hydrothermal condition; ZnO film

1. Introduction

Diluted magnetic semiconductors (DMSs) are currently attracting an intense interest as potential spintronic materials and are expected to play an important role in opto- and magneto-electronics devices. Among DMS materials, transition metal (TM) doped II–VI and III–V semiconductors [1–5] or III-Mn-V semiconductors such as $Ga_{1-x}Mn_xAs$ [1,6] and $In_{1-x}Mn_xAs$ [7] have been intensively studied. These materials are known to present ferromagnetic behaviour but their low Curie temperature, around 110 K have hindered their importance.

More recently a particular attention was given to the wide band gap würtzite phase ZnO semiconductor. Theoretical predictions indicated the possibility to obtain room temperature ferromagnetism after a partial substitution of Zn by magnetic ions in the ZnO structure [8–11]. Experiments on thin films of ZnO:TM have already been the subject of a large number of publications.

Several groups have studied the growth of Co-doped ZnO thin films. Pulsed laser deposited samples showed ferromagnetic behaviour [12] with a Curie temperature higher than room temperature.

Lee et al. [13] reported ferromagnetism above 350 K in Co-doped ZnO films synthesized by sol–gel technique. Laser molecular beam epitaxy has been used by Jin et al. [14] to grow ZnO:Co films with 1 mol% of Al on sapphire. Optical studies confirm that Co is divalent, high spin, and substituting for Zn. Ferromagnetism was also reported by Lim et al. [15] in $Zn_{1-x}Co_xO$ ($0.02 < x < 0.40$) films grown on Al_2O_3 substrates by the radio-frequency (rf) magnetron co-sputtering method.

More recently, Co-doped ZnO films with a Curie temperature far above 300 K and prepared by reactive sputtering have been reported by Dinia et al. [16] to be ferromagnetic. All the reported results have revealed that Zn^{2+} can be substituted by Co^{2+} in the ZnO matrix up to 25%. However, the magnetic signal was very small, below 1 μ_B/Co atom, which makes the experimental measurements very

* Corresponding author. Tel.: +333 88 10 70 67; fax: +333 88 10 72 49.
E-mail address: aziz.dinia@ipcms.u-strasbg.fr (A. Dinia).

0920-5861/$ – see front matter © 2005 Elsevier B.V. All rights reserved.
doi:10.1016/j.cattod.2005.11.073

inaccurate. The determination of the precise nature of the magnetic coupling is therefore difficult.

In order to increase the magnetic signal and to identify the origin of the magnetism in these compounds, it seems interesting to elaborate Co-doped ZnO in a bulk form. Nevertheless, very few studies attempt the elaboration of ZnCoO polycrystalline powders.

Deka et al. [17] have successfully synthesized nanocrystalline $Zn_{1-x}Co_xO$ powders using an auto-combustion method and have shown that ferromagnetism up to 770 K is observed for small concentrations of Co ($x < 0.1$).

With a standard solid state reaction, Han et al. [18] have also produced $Zn_{1-x}Co_xO$ polycrystalline powders. The samples with $x < 0.2$ remained paramagnetic down to 2 K and no sign of ferromagnetism was observed.

By hydrolysis in a polyol medium method [19], $Zn_{1-x}Co_xO$ würtzite like particles were obtained in a large composition range (from $x = 0$ to 0.65).

Ferromagnetism with $T_C > 350$ K was observed in aggregated nanocrystals of Co^{2+}:ZnO elaborated by hydrolysis and condensation in DMSO solvent at room temperature [20].

In this paper we present our contribution concerning the synthesis of $Zn_{1-x}Co_xO$ in polycrystalline form by a hydrothermal technique, which has already been used for the elaboration of pure ZnO powders [21–24] but never for Co-doped ZnO. The aim is to present the influence of the acetate and KOH concentrations on the properties of the ZnCoO samples and to determine the highest amount of Co that can be inserted in the ZnO structure.

2. Experimental

2.1. Sample preparation

The hydrothermal method is a wet chemical method which is used for preparing powders. Well crystallized particles, phase homogeneity and controlled particle morphology can be produced by this technique. The Co-doped ZnO powder was prepared under hydrothermal conditions as follows: dihydrated zinc acetate ($Zn(CH_3COO)_2{\cdot}2H_2O$) and tetrahydrated cobalt acetate ($Co(CH_3COO)_2{\cdot}4H_2O$) were co-precipitated by KOH in aqueous solution.

The mixture was sealed and hydrothermally reacted at 240 °C for 16 h. The precipitates obtained after this treatment were filtered, washed with distilled water and absolute ethanol and dried at 40 °C. Four series of samples have been prepared in order to optimise the synthesis conditions as reported in Table 1. In the first series, both the Co content and the total acetate concentration have been fixed at 2 at.% and 0.5 mol/L, respectively, and we investigated the effect of the KOH base concentration. In the second and third series we used the highest and the lowest values in the optimised KOH concentration range (2.5 and 0.77 mol/L) and we varied the Co concentration. Finally, in the last series we fixed both the optimised Co content and the base concentration and we investigated the role of the acetate concentration.

2.2. Physical measurements

X-ray diffraction (XRD) spectra were collected in the θ–2θ mode between 30° and 85°, using a Siemens D-500 instrument equipped with a Co target ($\lambda_{Co} = 1.789$ Å).

The cationic composition of the samples was checked by means of inductive coupled plasma (ICP).

Absorbance spectra were obtained using a Lambda 19 ultraviolet–visible spectrometer. A step width of 240 nm/mn was used to record the spectra between 200 and 2500 nm. The measurements have been performed at room temperature.

Magnetic measurements were performed using a superconducting quantum interference device (SQUID) magnetometer both at room and low temperatures (4 K).

3. Results and discussion

All the prepared samples were moss green for small Co concentration and became darker with increasing Co contents.

We first investigated the influence of the base concentration [KOH] while the Co content and total acetate concentration [Ac] were fixed at 2 at.% and 0.5 mol/L, respectively (series 1). The typical XRD patterns of Co-doped ZnO powder obtained using different KOH concentrations are shown in Fig. 1. For [KOH] $\leq$ 0.7 mol/L, the diffraction patterns reveal the presence of peaks corresponding to the hexagonal ZnO structure with additional peaks attributed to the Co_3O_4 spinel phase. For samples with [KOH] > 0.7 mol/L there is no indication of any parasitic or additional phase and only the expected peak positions for the würtzite ZnO structure are observed. This indicates that in the following base concentration range [0.7, 2.5 mol/L] the ZnCoO adopts a pure würtzite phase. Therefore, we have studied the effect of the cobalt content within the limits of the base concentration interval [0.7, 2.5 mol/L].

In the case [KOH] = 2.5 mol/L (series 2), X-ray diffraction data obtained on samples with different amounts of Co in $Zn_{1-x}Co_xO$ ($x = 0$, 0.02, 0.10, 0.20, 0.25) and ([Ac] = 0.5 mol/L) are shown in Fig. 2. The spectrum of pure ZnO phase is always reported for comparison. For the sample with $x = 0.10$,

Table 1
Experimental conditions used for the sample preparation

Samples	$Zn_{1-x}Co_xO$	[Ac] (mol/L) ([Zn Ac_2, $2H_2O$] + [$CoAc_2$, $4H_2O$])	[KOH] (mol/L)
Series 1	$x = 0.02$	0.5	0.14, 0.20, 0.70, 1.13, 2.50
Series 2	$x = 0$, 0.02, 0.10, 0.20, 0.25	0.5	2.50
Series 3	$x = 0$, 0.10, 0.20, 0.25	0.5	0.77
Series 4	$x = 0.10$	0.1, 0.3, 0.5, 0.7, 0.9	0.77

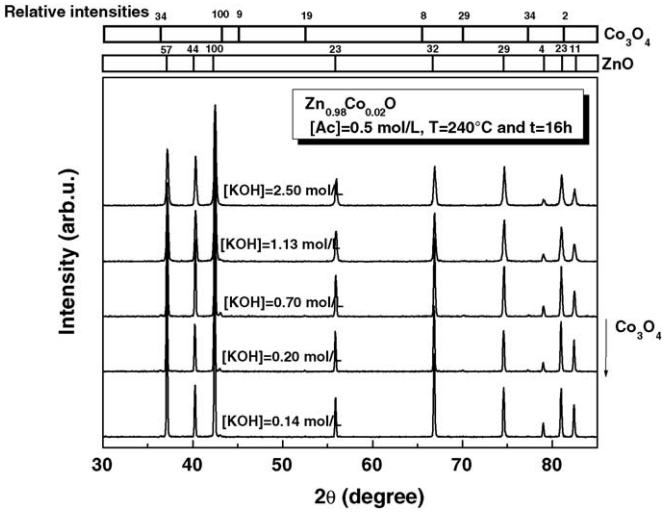

Fig. 1. θ–2θ X-ray diffraction patterns of ZnO and $Zn_{0.98}Co_{0.02}O$ polycrystalline powders obtained using different KOH concentrations (series 1).

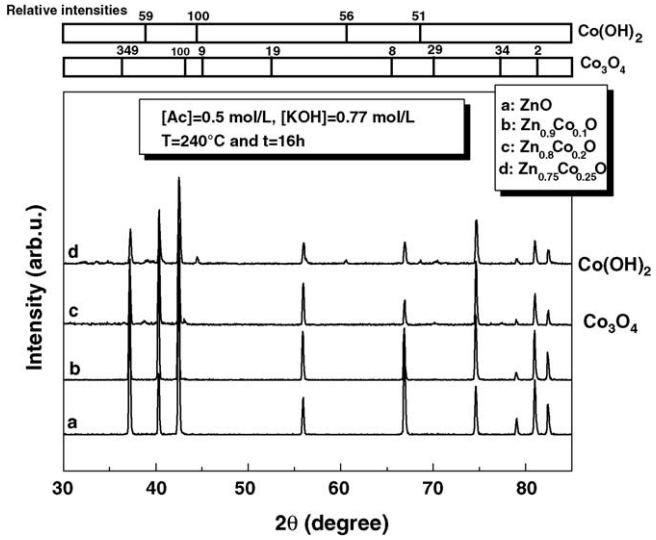

Fig. 3. θ–2θ X-ray diffraction patterns of polycrystalline powders presenting different amounts of Co in the ZnO matrix and obtained using KOH and acetate concentrations of 0.77 and 0.5 mol/L, respectively (series 3).

in addition to the diffraction peaks of the hexagonal ZnO phase, CoO phase peaks are observed. The amount of this secondary phase increases with increasing Co concentration and is the highest for 25 at.% of Co. However, for small Co concentration (2 at.%) the diffraction pattern reveals only the presence of the peaks corresponding to hexagonal ZnO and no second phase peaks, but this does not allow to exclude the possibility to form CoO clusters small enough to be detected by XRD.

The influence of the Co concentration has been also studied for the lower limit of the base concentration [KOH] = 0.77 mol/L (series 3). Powder X-ray diffraction XRD patterns of the as-synthesized samples obtained with different amounts of Co in $Zn_{1-x}Co_xO$ ($x = 0, 0.10, 0.20, 0.25$) and ([Ac] = 0.5 mol/L) are shown in Fig. 3. For $x \geq 0.20$, XRD patterns present the expected hexagonal würtzite structure with additional peaks that correspond to the presence of Co_3O_4 for $x = 0.20$ and to $Co(OH)_2$ for $x = 0.25$. The XRD pattern for $x = 0.10$ presents only the ZnO würtzite structure, undisturbed by the substitution of Co. No additional peaks due to any impurity are observed. The cell parameters of the würtzite-like phase remain almost constant and close to pure ZnO parameters ($a = 3.250(2)$ Å, $c = 5.207(7)$ Å). This was expected due to the similar values of ionic radii of Co^{2+} and Zn^{2+} cations [25]. To obtain the exact value of the Co concentration we used the inductive coupled plasma (ICP) technique, which gives a value of Co inserted in the ZnO matrix of $7.5 \pm 0.5\%$, smaller than the nominal one.

The average particle size for all ZnCoO samples has been calculated from X-ray line broadening using the Scherrer formula: $D = 0.9\frac{\lambda}{\beta \cos\theta}$, where D is the particle diameter, β the full width at half-maximum in radian, θ the angle of the diffraction peak and λ is the X-ray wavelength. We obtain an average value of 100 nm.

The influence of the total acetate concentration has also been studied for the optimised 10 at.% CO sample (series 4). XRD patterns of the as-synthesized samples obtained for $Zn_{0.9}Co_{0.1}O$ with [KOH] = 0.77 mol/L and different concentration of acetates are reported in Fig. 4. For all the acetate concentrations the ZnO würtzite phase is well observed. In addition to the peaks of the ZnO phase, the spectra present additional peaks corresponding to Co_3O_4 phase for [Ac] > 0.5 mol/L or to $Co(OH)_2$ phase for [Ac] < 0.5 mol/L. However for [Ac] = 0.5 mol/L, the powder is well crystallized in the hexagonal würtzite structure without any parasitic phase.

In order to support the XRD results and to confirm that tetrahedral Co^{2+} ions are well substituted to Zn^{2+}, we have used UV–vis spectroscopy. In tetrahedral symmetry, for a Co^{2+} cation in $3d^7$ configuration, the fundamental state is $^4A_2$ (F). For this configuration there are three allowed transitions from the $^4A_2$ (F) fundamental state towards the $^4T_2$ (F), $^4T_1$ (F) and $^4T_1$ (P) states. The first one, $\nu_1(Co_{Td}{}^{2+})$: $^4T_2$ (F) ← $^4A_2$ (F), occurs in IR field [26]. The transition bands, $\nu_2(Co_{Td}{}^{2+})$: $^4T_1$

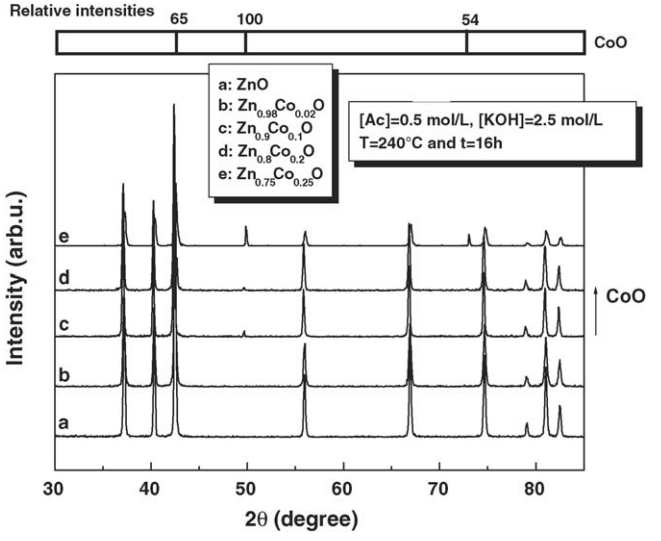

Fig. 2. θ–2θ X-ray diffraction patterns of polycrystalline powders presenting different amounts of Co in the ZnO matrix and obtained using KOH and acetate concentrations of 2.50 and 0.5 mol/L, respectively (series 2).

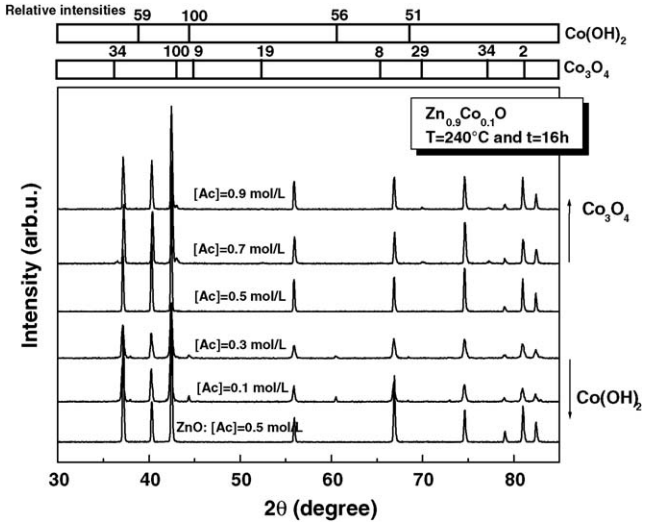

Fig. 4. X-ray diffraction patterns for $Zn_{0.9}Co_{0.1}O$ polycrystalline powders as a function of acetate concentrations with [KOH] = 0.77 mol/L (series 4).

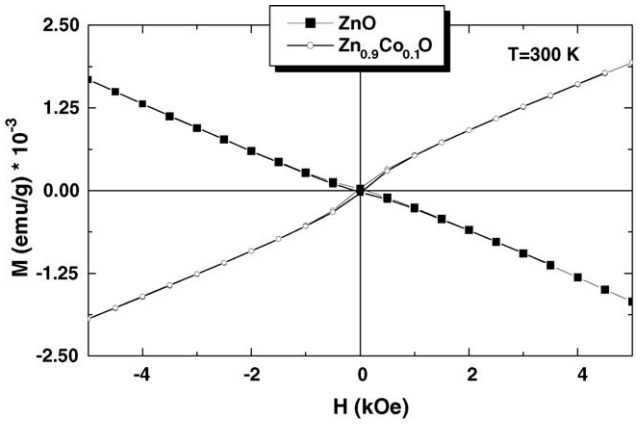

Fig. 6. Room temperature magnetization loops of ZnO and $Zn_{0.9}Co_{0.1}O$ polycrystalline powders.

(F) ← $^4A_2$ (F) and $\nu_3(Co_{Td}{}^{2+})$: $^4T_1$ (P) ← $^4A_2$ (F), are often presented in Near Infra Red and visible fields, respectively [27].

Fig. 5 shows optical absorbance spectral of ZnO and $Zn_{0.925}Co_{0.075}O$ polycrystalline powders synthesised with [KOH] = 0.77 mol/L and [Ac] = 0.5 mol/L. The absorption bands observed on the $Zn_{0.9}Co_{0.1}O$ spectrum in the visible and near IR fields: 15 408, 16 393, 17 699 and 6079, 7112, 7639 cm^{-1} correspond respectively to the transition bands, $\nu_3(Co_{Td}{}^{2+})$: $^4T_1$ (P) ← $^4A_2$ (F) and $\nu_2(Co_{Td}{}^{2+})$: $^4T_1$ (F) ← $^4A_2$ (F) and are attributed to d–d transitions of tetrahedral coordinated Co^{2+} according to reference [27].

Fig. 5 also shows a characteristic spectrum of pure ZnO phase with an absorption edge observed at 3.3 eV that corresponds to the band gap E_g for ZnO. This absorption edge is shifted towards lower energy (3 eV) for the $Zn_{0.9}Co_{0.1}O$ (spectrum b) sample. The redshift of the E_g edge with inserting Co in ZnO matrix has been already observed [28] and explained as mainly due to sp–d exchange interactions between the band electrons and the localized d electrons of the Co^{2+} ions substituting for Zn^{2+} ions [29,30]. The s–d and p–d exchange interactions give rise to a negative and a positive correction to the conduction-band and valence-band edges, respectively, leading to a narrowing of the band gap [31].

The magnetic properties of the powders are investigated using superconducting quantum interference device (SQUID). Fig. 6 shows the magnetization loop $M = f(H)$ of the pure ZnO and $Zn_{0.9}Co_{0.1}O$ polycrystalline powders measured at room temperature. The pure ZnO powder presents a diamagnetic behaviour. The doped sample remains paramagnetic down to 4 K and no sign of ferromagnetism is observed. Fig. 7 shows the comparison of a Brillouin function calculated for a system $S = 3/2$ and $g = 2$ with the signal measured for $Zn_{0.9}Co_{0.1}O$ at 4 K. It reveals that the sample magnetically behaves as an ideal paramagnet with no magnetic interactions. Considering that the ferromagnetism behaviour in diluted magnetic semi-conductors is due to the exchange interactions between free delocalized carriers (hole or electrons in the valence band) and the localized d spins on the transition metal ions, we

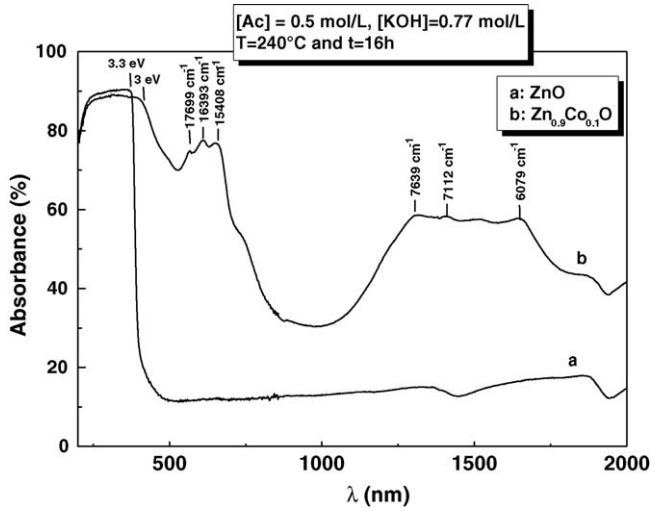

Fig. 5. Room temperature optical absorbance spectra of ZnO and $Zn_{0.9}Co_{0.1}O$ polycrystalline powders.

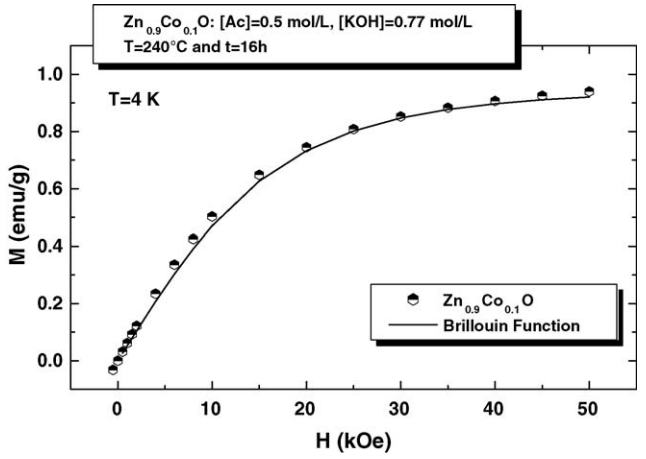

Fig. 7. Comparison between low temperature (4 K) magnetization loop of the $Zn_{0.9}Co_{0.1}O$ polycrystalline powder and a Brillouin function obtained using $S = 3/2$ and $g = 2$.

conclude that the presence of Co^{2+} in substitution for Zn^{2+} is not a sufficient condition for the observation of ferromagnetism. The presence of free carriers is a necessary condition for the appearance of a ferromagnetic behaviour. We can then conclude that our samples have a limited number of impurities or defects which may generate free carriers and consequently ferromagnetism.

4. Conclusion

In summary, we have succeeded to prepare a pure $Zn_{1-x}Co_xO$ powder by controlling the synthesis conditions and we have studied the structural and the magnetic properties of Co-doped ZnO polycrystalline samples produced by hydrothermal technique.

We showed that the acetates and KOH concentrations play an important role on the amount of Co that can be inserted in the ZnO matrix and on the presence of parasitic phases. The highest amount of Co^{2+} that we substituted for Zn^{2+} in the ZnO würtzite structure is about 10%. Magnetisation measurements performed at room temperature have shown paramagnetic behaviour for Co-doped ZnO samples with no evidence of ferromagnetism.

Reference

[1] H. Ohno, Science 281 (1998) 951.
[2] A. Twardowski, H.J.M. Swagten, W.J.M. de Jonge, Phys. Rev. B 36 (1987) 7013.
[3] T. Fukumura, Z. Jin, A. Ohtomo, H. Koinuma, M. Kawasaki, Appl. Phys. Lett. 75 (1999) 3366.
[4] W. Prellier, A. Fouchet, B. Mercey, J. Phys. Condens. Matter 15 (2003).
[5] S.A. Wolf, D.D. Awschalom, R.A. Buhrman, J.M. Daughton, S. von Molnar, M.L. Roukes, A.Y. Chtchelkanova, D.M. Treger, Science 294 (2001) 1488.
[6] H. Ohno, J. Magn. Mater. 200 (1999) 110.
[7] H. Ohno, H. Munekata, T. Penney, S. Molnar, L.L. von Chang, Phys. Rev. Lett. 68 (1992) 2664.
[8] K. Sato, H. Katayama-Yoshida, Jpn. J. Appl. Phys. 39 (2000) 555.
[9] K. Sato, H. Katayama-Yoshida, Semicon. Sci. Technol. 17 (2002) 367.
[10] T. Dietl, H. Ohno, F. Matsukura, J. Cibert, D. Ferrand, Science 287 (2000) 1019.
[11] T. Dietl, H. Ohno, F. Matsukura, Phys. Rev. B 63 (2001) 195.
[12] K. Ueda, H. Tabat, T. Kawai, Appl. Phys. Lett. 79 (2001) 988.
[13] H.J. Lee, S.Y. Jeong, C.R. Cho, C.H. Park, Appl. Phys. Lett. 81 (2002) 4020.
[14] Z.-W. Jin, T. Fukumura, K. Hasegawa, Y.-Z. Yoo, K. Ando, T. Sekiguchi, P. Ahmet, T. Chikyow, T. Hasegawa, H. Koinuma, M. Kawasaki, J. Cryst. Growth 237–239 (2002) 548.
[15] S.-W. Lim, D.-K. Hwang, J.-M. Myoung, Solid State Commun. 125 (2003) 231.
[16] A. Dinia, G. Schmerber, V. Pierron-Bohnes, C. Mény, P. Panissod, E. Beaurepaire, J. Magn. Magn. Mater. 286 (2005) 37.
[17] S. Deka, R. Paricha, P.A. Joy, Chem. Mater. 16 (7) (2004) 1168.
[18] S.-J. Han, B.Y. Lee, J.-S. Ku, Y.B. Kim, Y.H. Jeong, J. Mag. Mag. Mater. 272–276 (2004) 2008.
[19] L. Poul, S. Ammar, N. Jouini, F. Fiévet, F. Villain, Solid State Sci. 3 (2001) 31.
[20] D.-A. Schwartz, N.-S. Norberg, Q.-P. Nguyen, J.-M. Parker, D.-R. Gamelin, J. Am. Chem. Soc. 125 (2003) 13205.
[21] W.-J. Li, Er.-W. Shi, T. Fukuda, Cryst. Res. Technol. 38 (10) (2003) 847.
[22] H.-Y. Xu, H. Wang, Y.-C. Zhang, S. Wang, M.-K. Zhu, H. Yan, Cryst. Res. Technol. 38 (6) (2003) 429.
[23] B. Cheng, E.-T. Samulski, Chem. Commun. (2004) 986.
[24] K. Sue, K. Kimura, M. Yamamoto, K. Arai, Mater. Lett. 58 (2004) 3350.
[25] Y.Z. You, Fukumura, Z. Jin, K. Hasegawa, M. Kawazaki, P. Ahmet, T. Chikyow, H. Koinuma, J. Appl. Phys. 90 (2001) 4246.
[26] Lo. Jacono, A. Climino, C.A. Schuit, Gazzetta Chimica Italiana 103 (1973) 1281.
[27] A.A. Verberckmoes, B.M. Weckuysen, R.A. Schoonheydt, Micropor. Mesopor. Mater. 22 (1) (1998) 1165.
[28] K.J. Kim, Y.R. Park, Appl. Phys. Lett. 81 (2002) 1420.
[29] K. Ando, H. Saito, Z. Jin, T. Fukumura, M. Kawasaki, Y. Matsumoto, H. Koinuma, J. Appl. Phys. 89 (2001) 7284.
[30] Y.D. Kim, S.L. Cooper, M.V. Klein, B.T. Jonker, Phys. Rev. B 49 (1994) 1732.
[31] Y.R. Lee, A.K. Ramdas, R.L. Agarwal, Phys. Rev. B 38 (1988) 10600.